

Optimal biasing and physical limits of DVS event noise

Rui Graca, Brian McReynolds, Tobi Delbruck

Sensors Group, Inst. of Neuroinformatics, UZH-ETH Zurich, Zurich, Switzerland

rprgraca,bmac,tobi@ini.uzh.ch, <https://sensors.ini.uzh.ch>

Abstract—Under dim lighting conditions, the output of Dynamic Vision Sensor (DVS) event cameras is strongly affected by noise. Photon and electron shot-noise cause a high rate of non-informative events that reduce Signal to Noise ratio. DVS noise performance depends not only on the scene illumination, but also on the user-controllable biasing of the camera. In this paper, we explore the physical limits of DVS noise, showing that the DVS photoreceptor is limited to a theoretical minimum of 2x photon shot noise, and we discuss how biasing the DVS with high photoreceptor bias and adequate source-follower bias approaches optimal noise performance. We support our conclusions with pixel-level measurements of a DAVIS346 and analysis of a theoretical pixel model.

I. INTRODUCTION

The **Dynamic Vision Sensor (DVS)** [1]–[4] is a neuromorphic event-based vision sensor, which consists of an array of asynchronously operating pixels as the one in Fig. 1 [4]. Each pixel independently encodes instantaneous changes in its input light into an asynchronous stream of ON and OFF events. More specifically, a pixel outputs an ON event when the relative **Temporal Contrast (TC)** [1] of light intensity at its input increases by a user defined ON threshold since the last event, or an OFF event when the relative **TC** increases by a user defined OFF threshold since the last event. When its input is static, a **DVS** pixel ideally outputs no event. More extensive description of the **DVS** pixel operation can be found in [1], [5], [6].

Characteristics of the **DVS** such as sparse data encoding and low latency make it a good candidate for scientific applications such as space situational awareness and wide-field voltage and calcium imaging. The adequacy of the **DVS** for some applications is potentially limited by a too high rate of parasitic **Background Activity (BA)**. **BA** consists of events that do not encode changes in the input. These events are undesirable because they decrease the **Signal-to-Noise Ratio (SNR)** and increase data volume [5], [8]. The **BA** of the **DVS** pixel strongly depends on both light intensity and camera biasing [3], [6], [9]–[11]. It is predominantly caused by photon and electron shot noise in dark settings [9], and by leakage in the reset transistor (Fig. 1F) in brighter settings [10].

A good understanding of the phenomena resulting in **BA** is important for improving camera models that can aid pixel design, optimization of the camera utilization, or learning algorithms [5], [6], [12], [13].

In [9], noise power at the output of the photoreceptor (V_{pr} in Fig. 1) and noise event rate are explored as a function of

illumination and photoreceptor bias I_{pr} . There, we observe that both noise power and event rate are lower for lower I_{pr} . This occurs because the bandwidth is lower for lower I_{pr} .

These observations suggest that using a small I_{pr} to limit bandwidth reduces noise, and this assumption has been used as an optimization rule for bias control [13]. In this paper, we go a step further into understanding the optimal conditions and biasing of the **DVS** pixel, and show that in fact the opposite is generally true – even though strongly reducing I_{pr} leads to a decrease in noise events, noise performance is more optimal for high I_{pr} . We show that the **DVS** photoreceptor topology is bounded with a theoretical minimum of 2x photon shot noise, and we discuss bias optimization regarding bandwidth and its implications on noise and signal. In this paper, we focus on the biasing of the photoreceptor (Fig. 1A) by I_{pr} and the **Source-Follower buffer (SF)** (Fig. 1B) by I_{sf} . A more general discussion about bias optimization is presented in [6], and considerations about threshold and refractory biases are discussed in [11].

II. OPTIMAL PHOTORECEPTOR BIASING

A. PSD Measurements and modeling

Fig. 2a shows the noise **PSD** measured at V_{pr} of a test pixel isolated from a DAVIS346 array under an on-chip illuminance of 0.1 lx for two different I_{pr} settings: one high (3 nA) and one low (10 pA). The dashed lines in the figure show the **PSD** predicted by a theoretical physically-realistic model operating under the same conditions. The theoretical model was obtained by circuit analysis considering the sources of shot noise in the photoreceptor and applying the transfer function that relates them to V_{pr} . The parameters for the model were then estimated and fitted based on SPICE simulation and pixel measurements.

Since the theoretical model generally matches both measured and simulated data, we utilize it to further infer about the noise contribution of each noise source to the total output noise. In Fig. 2b, we see how the contribution of the photocurrent I_{pd} (depicted by the dotted lines and consisting of photon shot noise at the photodiode and electron shot noise added by M_{fb}) and the contribution of I_{pr} (depicted by the dashed lines, and consisting of noise introduced by M_n and the transistor implementing I_{pr}) add up to the total **PSD**. Here, we observe that the level of the contribution of I_{pd} is independent of I_{pr} , but its bandwidth may depend on I_{pr} – for a bias of 10 pA, I_{pr} is right at the edge of starting to filter out the I_{pd} contribution. That is, this contribution would be

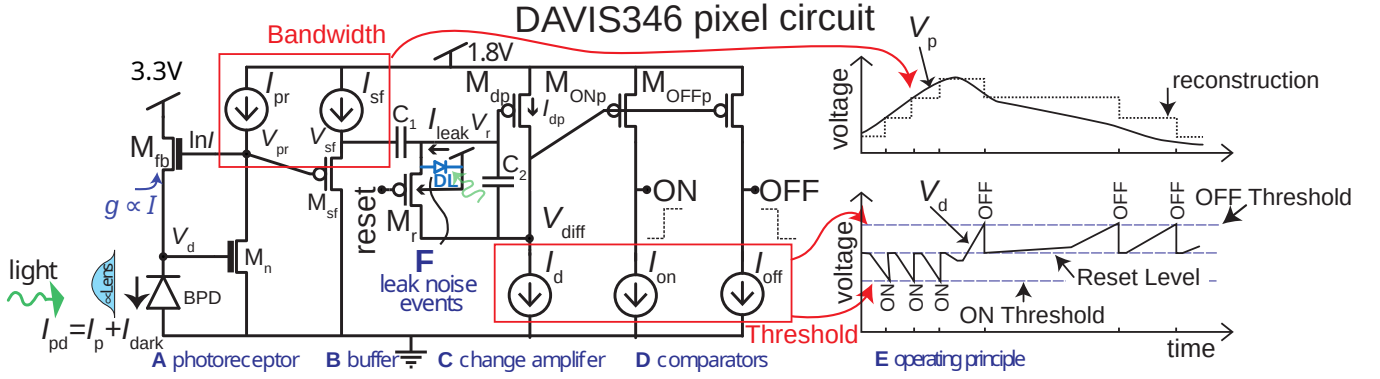


Fig. 1. Typical DVS pixel circuit [7]. The active logarithmic photoreceptor (A) is buffered by a source-follower (B), which drives a cap-feedback change amplifier (C), which is reset on each event by a low-going *reset* pulse. A finite refractory period holds the change amplifier in reset for the refractory period Δ_{refr} . Comparators (D) detect ON and OFF events as seen in E. Periodic leak events result from junction and parasitic photocurrent I_{leak} in diode DL (F).

significantly reduced for lower I_{pr} , and would become constant for higher I_{pr} (as happens for I_{pr} of 3 nA. On the other hand, the contribution of I_{pr} moves to higher frequencies when I_{pr} increases.

Fig. 2c shows the square root of the integral of the different components of the PSD in Fig. 2b. The final value of the square root of the integral is the RMS voltage noise contribution of its respective source. We see that the contribution of I_{pr} converges to a value independent of I_{pr} - the contribution is only shifted to higher frequencies. The contribution of I_{pd} is lower for lower I_{pr} , which happens due to filtering by I_{pr} [9]. For higher values of I_{pr} , filtering would stop occurring and the contribution of I_{pd} converges to the constant value observed at I_{pr} of 3 nA.

Figs. 2e and 2f show the modeled PSDs and the square root of their integrals for the contributors at the output of the SF, V_{sf} . The PSDs were obtained by filtering the ones at V_{pr} using a model of the SF estimated by circuit inspection and simulation. Also, the noise contribution of I_{sf} is added in the dashed line. However, its value is much smaller than the contribution of the photoreceptor (the summation of the contributions of I_{pd} and I_{pr}).

Fig. 2d shows the modeled signal transfer function from logarithmic changes in light intensity to voltages at V_{pr} and V_{sf} . As described in [9], it can be approximately modeled as a second order system with one pole dependent on I_{pd} and the other dependent on I_{pr} . At I_{pr} of 3 nA, the pole controlled by I_{pd} is clearly dominant, while for I_{pr} of 10 pA the two poles lie very close to each other. The SF add another pole, which for the bias used is close to the dominant of the photoreceptor.

Fig. 3 show the noise rates measured from the same test pixel for varying I_{pr} for two different on-chip illumination levels. We observe that for high I_{pr} , noise rate becomes mostly constant, since all the noise components of I_{pr} are filtered out. For middle I_{pr} values, the noise contributions of I_{pr} lie within the signal bandwidth and are not filtered out, and the noise rates peak. For lower I_{pr} the noise rates decrease because I_{pr} limits the bandwidth.

B. Optimal biasing and optimality analysis

From Fig. 2c we can see how strongly biasing I_{pr} results in shifting the noise components added by I_{pr} to higher frequencies outside the bandwidth of interest for signal. This means that we can filter them out using the SF without consequences for signal. In the limit, if we bias I_{pr} so strongly that all its contribution is removed by SF, the output noise consists of only the noise contribution of I_{pd} (which consists itself on equal parts of photon shot noise and M_{fb} noise), and the much smaller noise contribution of I_{sf} . In this case, we are theoretically limited to a minimum of 2x photon shot noise when the contribution of I_{sf} becomes negligible.

The clear advantage of strongly biasing I_{pr} is illustrated in Fig. 2f. For I_{pr} of 3 nA, the model predicts a contribution of photon shot noise of 46% (approximating the theoretical limit of 50%), resulting in a noise event rate of 0.02 Hz under nominal threshold and refractory biases [6] versus 12% for I_{pr} of 10 pA, resulting in a noise event rate of 0.66 Hz.

The model predicts an RMS noise contribution equivalent to TC log-e units of 0.006 for I_{sf} . The contributions of I_{pd} and I_{pr} depend on filtering, but for the case where the pole controlled by I_{pd} is dominant and filtering by the SF is not considered, they are respectively 0.04 and 0.06 for most values of I_{pd} and I_{pr} . Although RMS noise alone is not enough to characterize DVS noise, since it does not contain information about the noise frequency [9], these numbers are useful to evaluate design limitations to the event sensitivity (i.e. the minimum event threshold with acceptable noise rates). One important conclusion is that I_{sf} should be adjusted to the minimum acceptable bandwidth for each application and I_{pr} should be adjusted so that all its contributions are filtered out. Given that increasing I_{pr} increases power consumption, I_{pr} should be optimized to trade off power with noise performance. In the limit where the photoreceptor bandwidth is much higher than the SF bandwidth (which happens for very high illuminance, high I_{pr} and nominal or low I_{sf}) the noise, noise introduced by I_{pd} and I_{pr} is filtered out and SF becomes the main noise contributor.

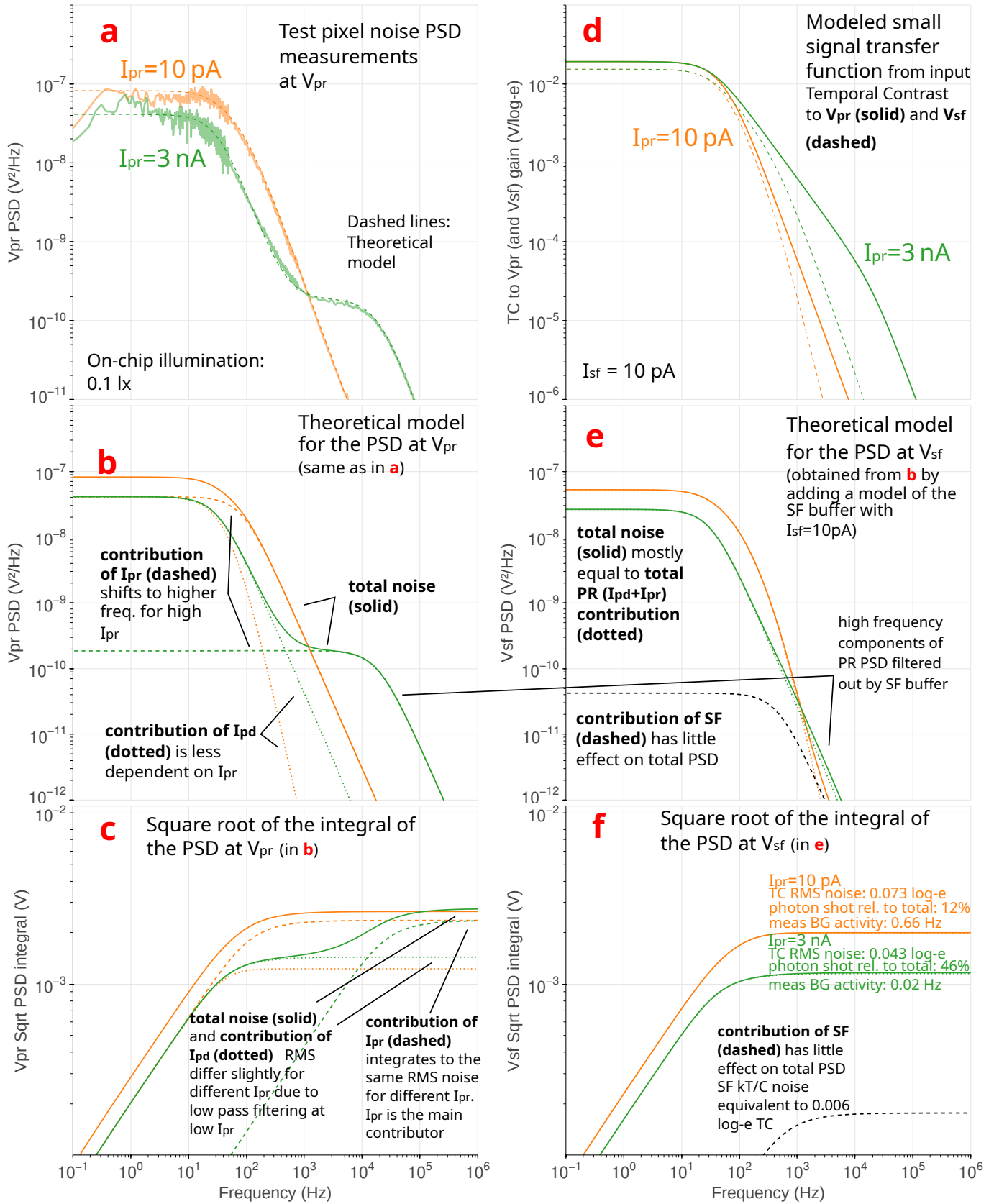


Fig. 2. (a) shows noise PSDs measured from a DAVIS346 test pixel for two different I_{pr} biases for an on-chip illuminance of 0.1 lx and the PSDs estimated by a theoretical model for the same conditions. (b) shows the estimated contributions of I_{pr} and I_{pd} to the total PSD for the same model in the same conditions, and (c) shows the square root of the integral of the curves in (b). The final value of these curves is the respective contribution to the RMS noise voltage at V_{pr} . (e) and (f) show the same quantities as (b) and (c), but relative to V_{sf} . (d) shows the estimated signal transfer function from TC (in log-e units) to V_{pr} and V_{sf} .

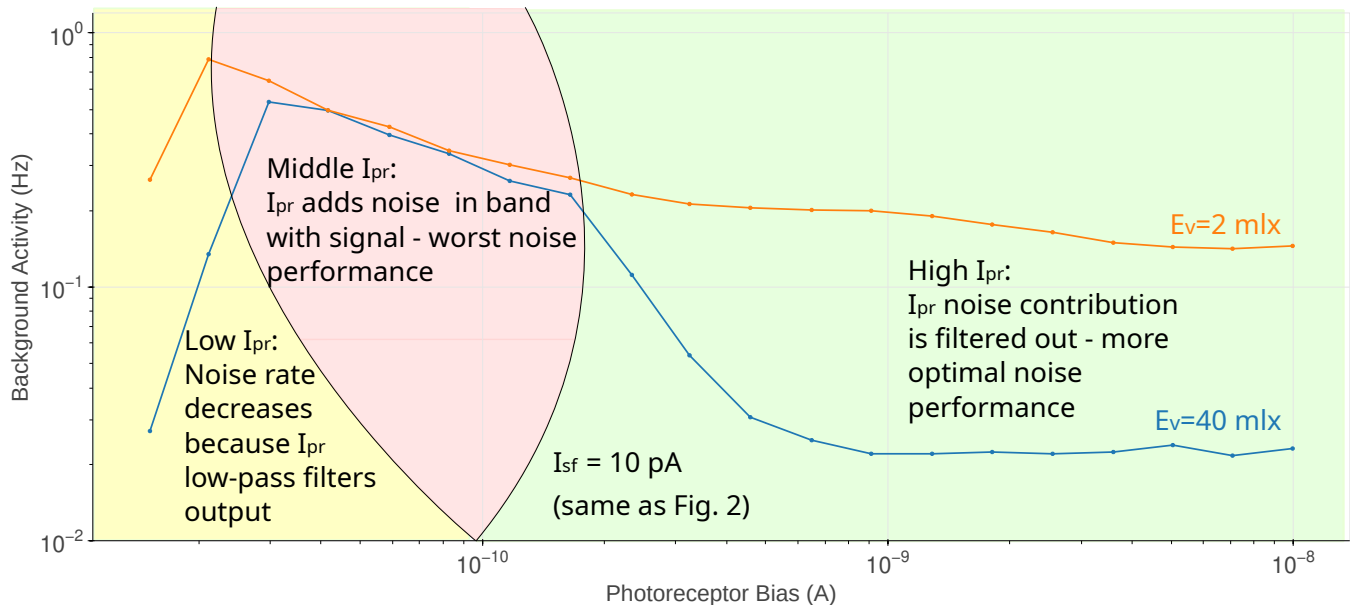


Fig. 3. Background activity measured from a DAVIS346 test pixel under constant on-chip illuminance of 2 mlx (orange line) and 40 mlx (blue line) for I_{sf} of 10 pA (as in Fig. 2) and nominal threshold and refractory bias settings (see [6] for a characterization of these parameters, nominal settings corresponds to tweaks of 0 there).

Filtering with **SF** and not with I_{pr} is generally a better idea since it introduces significantly less noise, and the noise it introduces is not filtered out in any case. However, in practical **DVS** implementations operating in very dark settings, very low I_{pr} may result in a lower bandwidth than the minimum achievable by the **SF**, and minimizing both I_{pr} and I_{sf} may result in less **BA**.

III. CONCLUSION

The measurements and analysis presented show that the **DVS** pixel is limited to a minimum of 2x photon shot noise, and that using high I_{pr} and adequate I_{sf} approximates this limit. We also discuss the limits imposed to event sensitivity by each noise contributor.

REFERENCES

- [1] P. Lichtsteiner, C. Posch, and T. Delbruck, "A 128 × 128 120 dB 15 μ s latency asynchronous temporal contrast vision sensor," *IEEE Journal of Solid-State Circuits*, vol. 43, no. 2, pp. 566–576, 2008.
- [2] Y. Suh, S. Choi, M. Ito, J. Kim, Y. Lee, J. Seo, H. Jung, D. H. Yeo, S. Namgung, J. Bong, S. Yoo, S. H. Shin, D. Kwon, P. Kang, S. Kim, H. Na, K. Hwang, C. Shin, J. S. Kim, P. K. J. Park, J. Kim, H. Ryu, and Y. Park, "A 1280 × 960 dynamic vision sensor with a 4.95- μ m pixel pitch and motion artifact minimization," in *2020 IEEE International Symposium on Circuits and Systems (ISCAS)*, 2020, pp. 1–5. DOI: [10.1109/ISCAS45731.2020.9180436](https://doi.org/10.1109/ISCAS45731.2020.9180436).
- [3] T. Finatou, A. Niwa, D. Matolin, K. Tsuchimoto, A. Mascheroni, E. Reynaud, P. Mostafalu, F. Brady, L. Chotard, F. LeGoff, H. Takahashi, H. Wakabayashi, Y. Oike, and C. Posch, "5.10 a 1280 × 720 back-illuminated stacked temporal contrast event-based vision sensor with 4.86 μ m pixels, 1.066GEPS readout, programmable event-rate controller and compressive data-formatting pipeline," in *2020 IEEE International Solid-State Circuits Conference - (ISSCC)*, 2020, pp. 112–114. DOI: [10.1109/ISSCC19947.2020.9063149](https://doi.org/10.1109/ISSCC19947.2020.9063149).
- [4] C. Brandli, R. Berner, M. Yang, S. Liu, and T. Delbruck, "A 240 × 180 130 dB 3 μ s latency global shutter spatiotemporal vision sensor," *IEEE Journal of Solid-State Circuits*, vol. 49, no. 10, pp. 2333–2341, 2014. DOI: [10.1109/JSSC.2014.2342715](https://doi.org/10.1109/JSSC.2014.2342715).

- [5] Y. Hu, S.-C. Liu, and T. Delbruck, "V2e: From video frames to realistic DVS events," in *Proceedings of the IEEE/CVF Conference on Computer Vision and Pattern Recognition (CVPR) Workshops*, Jun. 2021, pp. 1312–1321.
- [6] R. Graca, B. McReynolds, and T. Delbruck, "Shining light on the DVS pixel: A tutorial and discussion about biasing and optimization," in *2023 IEEE/CVF Conference on Computer Vision and Pattern Recognition Workshops (CVPRW)*, Jun. 2023. DOI: [10.48550/arXiv.2304.04706](https://doi.org/10.48550/arXiv.2304.04706).
- [7] G. Taverni, D. Paul Moeys, C. Li, C. Cavaco, V. Motsnyi, D. San Segundo Bello, and T. Delbruck, "Front and back illuminated dynamic and active pixel vision sensors comparison," *IEEE Transactions on Circuits and Systems II: Express Briefs*, vol. 65, no. 5, pp. 677–681, 2018.
- [8] S. Guo and T. Delbruck, "Low cost and latency event camera background activity denoising," *IEEE Transactions on Pattern Analysis and Machine Intelligence*, vol. 45, no. 1, pp. 785–795, 2023. DOI: [10.1109/TPAMI.2022.3152999](https://doi.org/10.1109/TPAMI.2022.3152999).
- [9] R. Graca and T. Delbruck, "Unraveling the paradox of intensity-dependent DVS pixel noise," in *2021 International Image Sensor Workshop (IISW)*, Sep. 2021. DOI: [10.48550/ARXIV.2109.08640](https://doi.org/10.48550/ARXIV.2109.08640).
- [10] Y. Nozaki and T. Delbruck, "Temperature and parasitic photocurrent effects in dynamic vision sensors," *IEEE Transactions on Electron Devices*, vol. 64, no. 8, pp. 3239–3245, Aug. 2017, ISSN: 1557-9646. DOI: [10.1109/TED.2017.2717848](https://doi.org/10.1109/TED.2017.2717848).
- [11] B. McReynolds, R. Graca, and T. Delbruck, "Exploiting alternating DVS shot noise event pair statistics to reduce background activity," in *2023 International Image Sensor Workshop (IISW)*, May 2023. DOI: [10.48550/arXiv.2304.03494](https://doi.org/10.48550/arXiv.2304.03494).
- [12] B. J. McReynolds, R. P. Graca, and T. Delbruck, "Experimental methods to predict dynamic vision sensor event camera performance," *Optical Engineering*, vol. 61, no. 7, p. 074 103, 2022. DOI: [10.1117/1.OE.61.7.074103](https://doi.org/10.1117/1.OE.61.7.074103).
- [13] T. Delbruck, R. Graca, and M. Paluch, "Feedback control of event cameras," in *2021 IEEE/CVF Conference on Computer Vision and Pattern Recognition Workshops (CVPRW)*, 2021, pp. 1324–1332. DOI: [10.1109/CVPRW53098.2021.00146](https://doi.org/10.1109/CVPRW53098.2021.00146).